

# Independent magnon states on magnetic polytopes

Jürgen Schnack, Heinz-Jürgen Schmidt<sup>1</sup>, Johannes Richter, Jörg  
Schulenburg<sup>2</sup>

<sup>1</sup> Universität Osnabrück, Fachbereich Physik, Barbarastr. 7, D-49069 Osnabrück, Germany

<sup>2</sup> Institut für theoretische Physik, Universität Magdeburg, P.O. Box 4120, D-39016 Magdeburg, Germany

Received: date / Revised version: date

**Abstract** For many spin systems with constant isotropic antiferromagnetic next-neighbour Heisenberg coupling the minimal energies  $E_{min}(S)$  form a rotational band, i. e. depend approximately quadratically on the total spin quantum number  $S$ , a property which is also known as Landé interval rule. However, we find that for certain coupling topologies, including recently synthesised icosidodecahedral structures this rule is violated for high total spins. Instead the minimal energies are a linear function of total spin. This anomaly results in a corresponding jump of the magnetisation curve which otherwise would be a regular staircase.

**Key words** independent magnons – magnetisation – geometric frustration

**PACS** 75.50.Xx, 75.10.Jm, 75.40.Cx

## 1 Introduction

It appears that for spin systems with constant isotropic antiferromagnetic next-neighbour Heisenberg exchange the minimal energy  $E_{min}(S)$  for given total spin quantum number  $S$  is typically a strictly convex function of  $S$ . For many spin topologies like rings, cubes, icosahedra etc. this function is very close to a parabola [1]. For certain systems this behaviour has been explained with the help of the underlying sublattice structure [2]. Experimentally this property has been described as “following the Landé interval rule” [3,4,5,6]. In the classical limit, where the single-spin quantum number  $s$  goes to infinity, the function  $E_{min}(S)$  is even an exact parabola if the system possesses co-planar ground states [7].

However, we find that for certain coupling topologies, including the cuboctahedron and the icosidodecahedron [8], this rule is violated for high total spins. More

---

Send offprint requests to: Jürgen Schnack

precisely, for the icosidodecadron the last four points of the graph of  $E_{min}$  versus  $S$ , i. e. the points with  $S = S_{max}$  to  $S = S_{max} - 3$ , lie on a straight line

$$E_{min}(S) = 60Js^2 - 6Js(30s - S). \quad (1)$$

An analogous statement holds for the last three points of the corresponding graph for the cuboctahedron. These findings are based on numerical calculations of the minimal energies for several  $s$  both for the icosidodecahedron as well as for the cuboctahedron. For both systems, additionally, we have a rigorous proof of the high spin anomaly for the case of  $s = 1/2$ . This proof rests on an inequality which says that all points of the graph of  $E_{min}$  versus  $S$  lie above or on the line connecting the last two points (“bounding line”). The proof can be easily applied to a wide class of spin systems, e.g. to two-dimensional spin arrays.

The observed anomaly – linear instead of parabolic dependence – results in a corresponding jump of the magnetisation curve  $\mathcal{M}$  versus  $B$ . In contrast, for systems which obey the Landé interval rule the magnetisation curve at very low temperatures is a staircase with equal steps up to the highest magnetisation.

The anomaly could indeed be observed in magnetisation measurements of the so-called Keplerate structure  $\{\text{Mo}_{72}\text{Fe}_{30}\}$  which is a recently synthesized magnetic molecule where 30  $\text{Fe}^{3+}$  paramagnetic ions (spins  $s = 5/2$ ) occupy the sites of a perfect icosidodecahedron and interact via isotropic, next-neighbour antiferromagnetic exchange [9]. Unfortunately, the magnetisation measurements [10, 11] performed so far suffer from too high temperatures which smear out the anomaly.

Nevertheless, it may be possible to observe truly giant magnetisation jumps in certain two-dimensional spin systems which possess a suitable coupling topology. In such systems the magnetisation jump can be of the same order as the number of spins, i.e. the jump remains finite – or is macroscopic – in the thermodynamic limit  $N \rightarrow \infty$ .

The article is organized as follows. In section 2 we introduce basic definitions and explain how the results have been obtained. In section 3 the high spin anomaly is discussed and proven for the case of  $s = 1/2$ . We provide an outlook in section 4.

## 2 Definitions and Numerics

The Heisenberg Hamilton operator of the investigated spin systems is

$$\begin{aligned} \tilde{H} &= \frac{1}{2} \sum_{(u,v)} J_{u,v} \tilde{\mathfrak{s}}(u) \cdot \tilde{\mathfrak{s}}(v) + g\mu_B B \tilde{S}_z \\ &= \frac{J}{2} \sum_{(u,v) \in \Gamma} \tilde{\mathfrak{s}}(u) \cdot \tilde{\mathfrak{s}}(v) + g\mu_B B \tilde{S}_z, \quad \tilde{S}_z = \sum_u \tilde{s}_z(u), \end{aligned} \quad (2)$$

where the exchange parameters  $J_{u,v}$  are considered as the components of a symmetric matrix  $\mathbb{J}$ , i.e. every bond is taken into account twice. In particular, we assume  $J_{u,v} \in \{J, 0\}$  and  $J > 0$  which corresponds to antiferromagnetic coupling. In equation (2),  $g$  is the spectroscopic splitting factor and  $\mu_B$  the Bohr magneton.

The vector operators  $\underline{s}(u)$  are the spin operators (in units of  $\hbar$ ) of the individual  $N$  paramagnetic ions with constant spin quantum number  $s$ . Because the matrix  $\mathbb{J}$  couples only next-neighbours (see Fig. 1) the second sum in (2) runs over the set  $\Gamma$  of all next-neighbour pairs  $(u, v)$  of spins of a single molecule at sites  $u$  and  $v$ .  $\Gamma$  can be regarded as the set of “edges” of the corresponding undirected graph describing the coupling scheme of the molecule. The “vertices” of the graph correspond to the spin sites  $1, 2, \dots, N$ . For each spin site  $u$  let  $\Gamma(u)$  denote the set of neighbours of  $u$ . Throughout this article we will assume that the number of neighbours per site is constant, say  $|\Gamma(u)| \equiv j$ . The “distance” between two spin sites  $u$  and  $v$  will be the minimal number of edges connecting  $u$  and  $v$  (similar to the Manhattan distance).

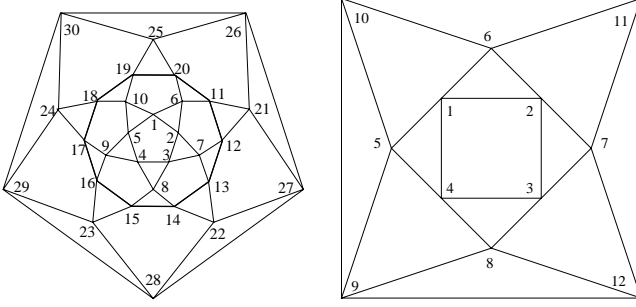


**Fig. 1** Planar projection of an icosidodecahedron (l.h.s.) and a cuboctahedron (r.h.s.) [8]. Solid lines denote couplings with a single exchange parameter  $J$ .

As mentioned already in the introduction the anomaly was found numerically. For this purpose the Hamilton matrix had to be diagonalized. The total matrix is a huge object of dimension  $(2s+1)^N \times (2s+1)^N$  which must be block-diagonalized in advance. Using that the Hamilton operator commutes with  $\underline{S}_z$ , the Ising product states which are a natural basis can be grouped according to the quantum numbers  $M$ , thereby dividing the Hilbert space into orthogonal subspaces  $\mathcal{H}(M)$ . A further reduction of dimension is achieved if the symmetries of the spin array are exploited. The icosidodecahedron for instance shows a tenfold shift symmetry leading to Hilbert subspaces  $\mathcal{H}(M, k)$  with  $k = 0, \dots, 9$ . Within these subspaces a Lanczos procedure was applied in order to obtain the respective minimal energies.

### 3 High spin anomaly

#### 3.1 Observations

The resulting minimal energies  $E_{min}(S)$  are shown by dashes on the l.h.s. of Fig. 2 for the icosidodecahedron and on the l.h.s. of Fig. 3 for the cuboctahedron. The straight lines denote the bounding lines, which connect the highest four levels in

the case of the icosidodecahedron and the highest three in the case of the cuboctahedron. At  $T = 0$  this behavior leads to jumps of the magnetisation  $\mathcal{M}$

$$\mathcal{M} = -\frac{1}{Z} \text{tr} \left\{ g\mu_B \tilde{S}_z e^{-\beta \tilde{H}} \right\}, \quad Z = \text{tr} \left\{ e^{-\beta \tilde{H}} \right\}. \quad (3)$$

Due to the effect that the states lie exactly on the bounding line in the graph of  $E_{min}$  versus  $S$  they “take over” for the new total ground state at the same value of the magnetic field, therefore the magnetisation immediately jumps to the highest value. The jumps are marked by arrows in the magnetisation curves of the icosidodecahedron (r.h.s. of Fig. 2) and the cuboctahedron (r.h.s. of Fig. 3).

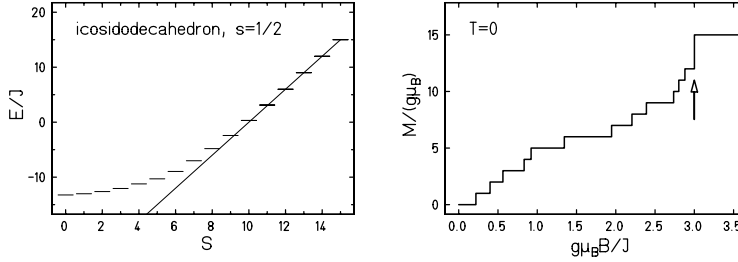


**Fig. 2** Icosidodecahedron: L.h.s. – minimal energy levels  $E_{min}(S)$  as a function of total spin  $S$ . R.h.s. – magnetisation curve at  $T = 0$ .

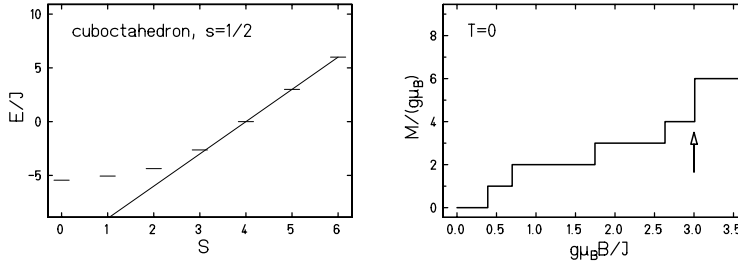


**Fig. 3** Cuboctahedron: L.h.s. – minimal energy levels  $E_{min}(S)$  as a function of total spin  $S$ . R.h.s. – magnetisation curve at  $T = 0$ .

For systems which follow the Landé interval rule, i.e. where  $E_{min}(S)$  is a parabolic function of  $S$ , the corresponding magnetisation curve would consist of equal steps.

### 3.2 Idea of the proof

A necessary condition for the anomaly is certainly that the minimal energy in the one-magnon space is degenerate. Therefore, localized one-magnon states can be

constructed which are also of minimal energy. When placing a second localized one-magnon eigenstate on the spin array there will be a chance that it does not interact with the first one if a large enough separation can be achieved. This new two-magnon state is likely the state of minimal energy in the two-magnon Hilbert space because for antiferromagnetic interaction two-magnon bound states do not exist (at least for  $s = 1/2$ ). This procedure can be continued until no further independent magnon can be placed on the spin array. In a sense the system behaves as if it consists of non-interacting bosons which, up to a limiting number, can condense into a single-particle ground state.

In more mathematical terms: In order to prove the high-spin anomaly we first show an inequality which says that all points  $(S, E_{min}(S))$  lie above or on the line connecting the last two points. This inequality holds for  $s = 1/2$  and all systems with constant antiferromagnetic exchange parameter and a constant number of neighbours for each spin site. For specific systems as those mentioned above what remains to be done is to construct particular states which exactly assume the values of  $E_{min}$  corresponding to the points lying on the bounding line, then these states are automatically states of minimal energy.

Note that the high spin anomaly does not contradict the strict convexity of the graph of  $E_{min}$  versus  $S$  in the classical limit, since in the limit  $s \rightarrow \infty$  the interval where the anomaly occurs, e. g.  $S = S_{max} - 3$  to  $S = S_{max}$ , becomes an infinitesimally small fraction of the total spin range.

We set  $J = 1$  throughout this section.

### 3.3 Bounding line for $s = 1/2$

Let  $\mathcal{H}_a$  denote the eigenspace of  $\mathcal{S}_z$  with eigenvalue  $M = N/2 - a$ ,  $a = 0, 1, \dots, N$ . It has the dimension  $\dim(\mathcal{H}_a) = \binom{N}{a}$ . An orthonormal basis of  $\mathcal{H}_a$  is given by the product states denoted by  $|n_1, \dots, n_a\rangle$  with  $1 \leq n_1 < n_2 < \dots < n_a \leq N$  where the  $n_i$  denote the sites with flipped spin  $m = -1/2$ . A state of this form will be called isolated iff  $(n_i, n_j) \notin \Gamma$  for all  $1 \leq i < j \leq a$ . In other words, the flipped sites of an isolated state must not be neighbours according to the coupling scheme.  $\mathcal{H}_a^{iso}$  will denote the subspace of  $\mathcal{H}_a$  spanned by isolated states.

We will embed the Hilbert space of the spin system into some sort of Fock space for magnons. More precisely, let  $\mathcal{B}_a(\mathcal{H}_1)$  be the totally symmetric (i. e. bosonic) subspace of  $\bigotimes_{i=1, \dots, a} \mathcal{H}_1$ . If  $A_1 : \mathcal{H}_1 \rightarrow \mathcal{H}_1$  is a linear operator,  $\mathcal{B}_a(A_1)$  will denote the restriction of  $A_1 \otimes \mathbb{1} \otimes \dots \otimes \mathbb{1} + \dots + \mathbb{1} \otimes \dots \otimes \mathbb{1} \otimes A_1$  onto  $\mathcal{B}_a(\mathcal{H}_1)$ . An orthonormal basis of  $\mathcal{B}_a(\mathcal{H}_1)$  is given by the bosonic states

$$\mathcal{S} |n_1\rangle \otimes \dots \otimes |n_a\rangle, \quad (4)$$

where  $1 \leq n_1 < n_2 < \dots < n_a \leq N$  and the ‘‘symmetrisator’’  $\mathcal{S}$  denotes the sum over all  $a!$  permutations of the product state divided by  $\sqrt{a!}$ . The linear extension

of the map  $|n_1, \dots, n_a\rangle \mapsto \mathfrak{S} |n_1\rangle \otimes \dots \otimes |n_a\rangle$  defines an isometric embedding

$$\mathcal{J}_a : \mathcal{H}_a \longrightarrow \mathcal{B}_a(\mathcal{H}_1). \quad (5)$$

Let  $\underline{H}_a$  denote the restriction of the Hamilton operator (2) (with zero magnetic field) onto  $\mathcal{H}_a$  and

$$\tilde{\underline{H}}_a \equiv \mathcal{J}_a^* \mathcal{B}_a(\underline{H}_1) \mathcal{J}_a. \quad (6)$$

We will show the following

**Proposition 1**  $\underline{H}_a = \frac{1-a}{8} Nj + \tilde{\underline{H}}_a$  if restricted to the subspace  $\mathcal{H}_a^{iso}$ .

$j$  is the number of neighbours, which is assumed to be constant for each spin site.

**Proof:** Let  $|n_1, \dots, n_a\rangle$  be an arbitrary isolated basis state and split  $\mathfrak{s}(u) \cdot \mathfrak{s}(v)$  into

$$\mathfrak{s}(u) \cdot \mathfrak{s}(v) = \mathfrak{s}_z(u) \mathfrak{s}_z(v) + \frac{1}{2} (\mathfrak{s}^+(u) \mathfrak{s}^-(v) + \mathfrak{s}^-(u) \mathfrak{s}^+(v)), \quad (7)$$

analogously  $\underline{H}_a = \underline{H}'_a + \underline{H}''_a$  and  $\tilde{\underline{H}}_a = \tilde{\underline{H}}'_a + \tilde{\underline{H}}''_a$ . First, let us consider

$$\begin{aligned} \underline{H}''_a |n_1, \dots, n_a\rangle &= \frac{1}{4} \sum_{(u,v) \in \Gamma} (\mathfrak{s}^+(u) \mathfrak{s}^-(v) + \mathfrak{s}^-(u) \mathfrak{s}^+(v)) |n_1, \dots, n_a\rangle \quad (8) \\ &= \frac{1}{4} \left( \sum_{m_1 \in \Gamma(n_1)} \text{Sort} |m_1, \dots, n_a\rangle + \dots + \sum_{m_a \in \Gamma(n_a)} \text{Sort} |n_1, \dots, m_a\rangle \right). \end{aligned}$$

Here Sort denotes the procedure which re-arranges a list of integers into its non-decreasing order. Note that further summation constraints of the form  $m_1 \neq n_2, \dots, n_a$  etc. would be superfluous since  $|n_1, \dots, n_a\rangle$  was assumed to be isolated. Now consider

$$\begin{aligned} \tilde{\underline{H}}''_a |n_1, \dots, n_a\rangle &= \mathcal{J}_a^* \mathcal{B}_a(\underline{H}''_1) \mathfrak{S} |n_1\rangle \otimes \dots \otimes |n_a\rangle \quad (9) \\ &= \frac{1}{4} \mathcal{J}_a^* \left( \sum_{m_1 \in \Gamma(n_1)} \mathfrak{S} |m_1\rangle \otimes \dots \otimes |n_a\rangle \right. \\ &\quad \left. + \dots + \sum_{m_a \in \Gamma(n_a)} \mathfrak{S} |n_1\rangle \otimes \dots \otimes |m_a\rangle \right) \\ &= \frac{1}{4} \left( \sum_{m_1 \in \Gamma(n_1)} \text{Sort} |m_1, \dots, n_a\rangle + \dots + \sum_{m_a \in \Gamma(n_a)} \text{Sort} |n_1, \dots, m_a\rangle \right) \\ &= \underline{H}''_a |n_1, \dots, n_a\rangle. \quad (10) \end{aligned}$$

Now we turn to  $\underline{H}'_a$ . Recall that there is a total number of  $L = \frac{Nj}{2}$  links between different sites. For a given basis state  $|n_1, \dots, n_a\rangle$  we write

$$L = L_{++} + L_{+-} + L_{--}, \quad (11)$$

where  $L_{++}$  denotes the number of links between two  $m = +1/2$ -sites, etc. Hence for isolated states  $L_{--} = 0$ . Each basis state is an eigenstate of  $\tilde{H}'_a$  with eigenvalue

$$\frac{1}{4}(L_{++} - L_{+-} + L_{--}) = \frac{1}{4}(L - 2L_{+-}). \quad (12)$$

For isolated states  $L_{+-} = ja$ , but in general  $L_{+-} = ja - 2L_{--}$  since each  $--$  link “deletes” two  $+-$  links of a corresponding isolated state. Hence

$$\tilde{H}'_a |n_1, \dots, n_a\rangle = \frac{1}{4} \left( \frac{Nj}{2} - 2ja + 4L_{--} \right) |n_1, \dots, n_a\rangle \quad (13)$$

$$= \frac{1}{4} \left( \frac{Nj}{2} - 2ja \right) |n_1, \dots, n_a\rangle. \quad (14)$$

Similarly one can show that

$$\tilde{H}'_a |n_1, \dots, n_a\rangle = \frac{a}{4} \left( \frac{Nj}{2} - 2j \right) |n_1, \dots, n_a\rangle. \quad (15)$$

From (15), (14), and (10) the proposition follows immediately.  $\blacksquare$

If we drop the condition that  $|n_1, \dots, n_a\rangle$  is isolated we ought to slightly modify our calculations. First, we would have to introduce extra summation constraints of the form  $m_1 \neq n_2, \dots, n_a$  etc. in (8) in order to be sure that the resulting states lie in  $\mathcal{H}_a$ . Although  $\mathcal{B}_a(\tilde{H}_1)$  in general will produce some unphysical states with two magnons localized at the same site, these states will be annihilated by  $\mathcal{J}_a^*$ . Hence again  $\tilde{H}''_a |n_1, \dots, n_a\rangle = \tilde{H}''_a |n_1, \dots, n_a\rangle$ .

For  $\tilde{H}'_a$  and  $\tilde{H}''_a$  the situation is different. The foregoing arguments show that the difference between the left and the right hand side of proposition 1 is some operator with eigenstates  $|n_1, \dots, n_a\rangle$  and corresponding eigenvalues  $L_{--}$  which are  $\geq 0$ . This shows that proposition 1 generalizes to

**Proposition 2**  $\tilde{H}_a \geq \frac{1-a}{8}Nj + \tilde{H}_a$ .

Now let  $E_a$  denote the smallest energy eigenvalue of  $\tilde{H}_a$ . Note that  $E_{\min}(S = N/2 - a) \geq E_a$ , since the energy eigenvalues for given total spin quantum number  $S$  are assumed within each subspace of magnetic quantum number  $M = -S, \dots, S$ . We expect that  $E_{\min}(S = N/2 - a) = E_a$  holds generally for the spin systems under consideration, this has been proven only for so-called bi-partite systems [12, 13], but numerically shown to hold for much more systems [14].

Analogously we define  $\tilde{E}_a$  for  $\tilde{H}_a$ . Since for bosons the ground state energy is additive,  $aE_1$  will be the smallest energy eigenvalue of  $\mathcal{B}(\tilde{H}_1)$ . We further conclude  $\tilde{E}_a \geq aE_1$  since  $\tilde{E}_a = \langle \Phi | \tilde{H}_a | \Phi \rangle = \langle \mathcal{J}_a \Phi | \mathcal{B}(\tilde{H}_1) | \mathcal{J}_a \Phi \rangle$  if  $\tilde{H}_a | \Phi \rangle = \tilde{E}_a | \Phi \rangle$ . Together with proposition 1 this implies

**Proposition 3**  $E_a \geq \frac{1-a}{8}Nj + aE_1$ .

This inequality says that the minimal energies  $E_a$ , resp.  $E_{\min}(S = N/2 - a)$ , lie above or on the “bounding line”  $\ell(a) = \frac{1-a}{8}Nj + aE_1$ .

### 3.4 Ground states of independent magnons

According to what has been said above in order to rigorously prove the high spin anomaly it suffices to construct states which assume the energy values of the bounding line  $\ell(a)$  for certain values of  $a > 1$ . By the results of the previous subsection it is clear that these energy values must be minimal and the states must be eigenstates of  $H_a$  in the case  $s = 1/2$ . Actually we conjecture that these states are also minimal energy states of  $H_a$  for arbitrary spin, which conjecture is numerically supported for all cases where we have calculated  $E_a$ , but we cannot prove it at the moment. Nevertheless, we will assume an arbitrary spin  $s$  in this subsection.

We first consider the case of the icosidodecahedron. Let  $a = 1$ . Recall that a general state in  $\mathcal{H}_a$  is of the form  $\sum_{n=1}^N c_n |n\rangle$ , where  $n$  denotes the spin site where the magnetic quantum number is decreased by 1. The eigenvalues of  $H_1$  are of the form

$$E_\alpha = \frac{1}{2} N j s^2 + (j_\alpha - j) s, \quad (16)$$

where  $j_\alpha, \alpha = 1, \dots, N$  are the eigenvalues of the coupling matrix  $\mathbb{J}$ . In our case,  $N = 30, j = 4$ , and the minimal eigenvalue  $j_\alpha$  is  $-2$ , hence

$$E_1 = 60s^2 - 6s. \quad (17)$$

The corresponding eigenspace of  $H_a$  is ten-fold degenerate. It is possible to find linear superpositions which are states of minimal energy and have some intuitive geometric interpretation as localized one-magnon states corresponding to even subrings of the icosidodecahedron. These states have alternating amplitudes  $c_n = \pm 1$  for sites  $n$  of the subring and vanishing amplitudes for the remaining sites. The smallest even subrings generating such states are the “8-loops” circumscribing two adjacent pentagons, e. g.  $(1, 2, 3, 4, 9, 17, 18, 10)$  according to the numbering of sites in Fig. 1 Other even subrings are the “equators” with 10 sites or the “curly equators” with 12 sites which need not be further considered here.

Now let  $a = 2$ . If a two-magnon ground state lies on the bounding line  $\ell(a)$ , as it is suggested by numerical diagonalization, we would have

$$E_2 = 60s^2 - 12s. \quad (18)$$

In fact, this energy is assumed by the following state: Consider two 8-loops  $L_1, L_2$  with a distance of 2, e. g.  $L_1 = (1, 2, 3, 4, 9, 17, 18, 10)$  and  $L_2 = (12, 13, 22, 28, 29, 30, 26, 21)$  according to Fig. 1.  $\epsilon_{n_1}, n_1 \in L_1$  and  $\delta_{n_2}, n_2 \in L_2$  denote the amplitudes which define the one-magnon ground-states described above. Then a two-magnon ground-state with the energy of (18) can be defined by

$$\Phi_2 = \sum_{n_1 \in L_1, n_2 \in L_2} \epsilon_{n_1} \delta_{n_2} |n_1, n_2\rangle. \quad (19)$$

Since this state lies entirely in  $\mathcal{H}_2^{iso}$  it can be considered as a ground-state of two non-interacting magnons.



**Table 1** Definition of an  $\mathcal{Y}_h$ -symmetric three-magnon ground-state by assignment of amplitudes to representative triple states.

$ n_1, n_2, n_3\rangle$	Length of orbit	Amplitude
$ 1, 3, 14\rangle$	60	1
$ 1, 3, 15\rangle$	120	-1
$ 1, 3, 22\rangle$	120	-1
$ 1, 3, 23\rangle$	120	1
$ 1, 3, 28\rangle$	120	1
$ 1, 3, 29\rangle$	60	-2
$ 1, 7, 15\rangle$	120	1
$ 1, 7, 18\rangle$	60	1
$ 1, 7, 23\rangle$	120	-1
$ 1, 7, 24\rangle$	120	-1
$ 1, 7, 29\rangle$	60	2
$ 1, 8, 21\rangle$	120	-1
$ 1, 8, 25\rangle$	30	2
$ 1, 8, 26\rangle$	120	-1
$ 1, 8, 27\rangle$	120	2
$ 1, 8, 28\rangle$	30	-2
$ 1, 13, 16\rangle$	20	-2
$ 1, 13, 24\rangle$	60	-1
$ 1, 13, 30\rangle$	60	2
$ 1, 14, 30\rangle$	20	-1

Unfortunately, an analogous construction of three mutually isolated one-magnon states is no longer possible for  $a = 3$ . Here we have to determine an appropriate state by numerical diagonalization. One possible state of three independent magnons is a state which is completely symmetric under the action of the symmetry group of the icosidodecahedron, i.e. the icosahedral group with reflections  $\mathcal{Y}_h$  of order 120. Hence it will suffice to define this state by assigning an amplitude to only one triple of sites within each orbit of the symmetry group. The other triples obtained by applying symmetry operations  $g \in \mathcal{Y}_h$  to each site will have, by definition, the same amplitude. The complete definition of this state (without normalization) can be found in Table 1. The calculation of the corresponding energy  $E_2 = 60s^2 - 18s$  can be done by a computer algebra software. Also this state lies entirely within  $\mathcal{H}_3^{iso}$ . Thus we have obtained a rigorous proof of the anomaly also for the case  $a = 3$  and  $s = 1/2$ .

The case of the cuboctahedron is largely analogous, up to the fact that here we have only one point of anomaly for  $a = 2$ . The corresponding two-magnon ground state can be constructed by using two separated 4-loops, e. g.  $(1, 2, 3, 4)$  and  $(9, 10, 11, 12)$  in Fig. 1 (r.h.s.).

### 3.5 Generalization to the XXZ-model

The above proof holds also for the more general Hamiltonian of the XXZ-model

$$\tilde{H} = \frac{J}{2} \sum_{(u,v) \in \Gamma} \left\{ \Delta \tilde{s}_z(u) \tilde{s}_z(v) + \tilde{s}_x(u) \tilde{s}_x(v) + \tilde{s}_y(u) \tilde{s}_y(v) \right\}, \quad (20)$$

with  $\Delta \geq 0$ . Since the total spin  $S$  is no longer a good quantum number, the minimal energies  $E_{min}$  have to be considered as a function of the total magnetic quantum number  $M$  instead. For the existence of the bounding line and the corresponding magnetisation jump this aspect is irrelevant. The only change in the proof is a multiplication of  $\tilde{H}'_a$  and  $\tilde{H}'_a'$  by  $\Delta$ , which does not change the argumentation. Also the construction of eigenstates, as carried out in subsection 3.4, is not altered by the anisotropy  $\Delta$  in (20), since these states are isolated.

## 4 Outlook

The shown proof offers a method to create spin arrays which by construction support a finite number of independent magnons. The basic idea is to design a unit cell which can host a localized one-magnon state, that is an eigenstate of the Hamiltonian. Triangles play a key role in the construction of such cells because they help to prevent localized magnons from escaping. The total spin array is then obtained by properly linking several unit cells. Fig. 4 shows an example. The unit cell is one quarter of the structure. It can host a single magnon

$$|1 \text{ magnon} \rangle = \frac{1}{2} (|1\rangle - |2\rangle + |3\rangle - |4\rangle), \quad (21)$$

which is an eigenstate of the Hamiltonian with minimal energy in the one-magnon space. One easily notices that in total four localized independent magnons fit into the structure. In general it might be possible that more independent magnons, like in the case of the icosidodecahedron, can occupy the spin array. For the example of Fig. 4 this is not the case.

The latter example offers the perspective of observing truly giant magnetisation jumps in two-dimensional spin systems. The number of independent magnons which can be placed on the lattice is proportional to the number of spins itself –  $N/6$  is the example of Fig. 4 – and thus a macroscopic quantity. This will be the subject of a forthcoming publication.

*Acknowledgements* J. Richter and J. Schulenburg thank the Deutsche Forschungsgemeinschaft for support (project Ri 615/10-1).

## References

1. J. Schnack, M. Luban, Phys. Rev. B **63** (2001) 014418
2. B. Bernu, P. Lecheminant, C. Lhuillier, L. Pierre, Phys. Rev. B **50** (1994) 10048

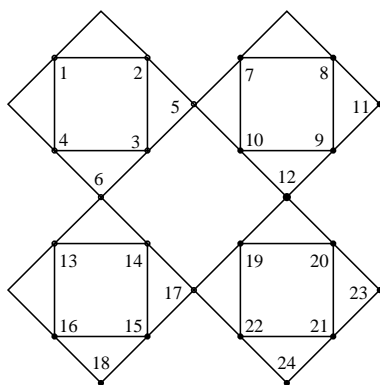


**Fig. 4** Fictitious two-dimensional spin array with periodic boundary conditions. This array hosts at least as many independent magnons as unit cells, i.e.  $4 \equiv N/6$ .

3. K. L. Taft, C. D. Delfs, G. C. Papaefthymiou, S. Foner, D. Gatteschi, S. J. Lippard, *J. Am. Chem. Soc.* **116** (1994) 823
4. A. Lascialfari, D. Gatteschi, F. Borsa, A. Cornia, *Phys. Rev. B* **55** (1997) 14341
5. A. Lascialfari, D. Gatteschi, F. Borsa, A. Cornia, *Phys. Rev. B* **56** (1997) 8434
6. G. L. Abbati, A. Caneschi, A. Cornia, A. C. Fabretti, D. Gatteschi, *Inorg. Chim. Acta* **297** (2000) 291
7. H.-J. Schmidt, M. Luban in preparation
8. H. S. M. Coxeter, *Regular Polytopes*, 3rd ed. (Dover, New York, 1973);  
Wolfram Research, <http://polyhedra.wolfram.com/archimedean/A01.html>,  
<http://polyhedra.wolfram.com/archimedean/A04.html>
9. A. Müller, S. Sarkar, S. Q. N. Shah, H. Bögge, M. Schmidtman, S. Sarkar, P. Kögerler, B. Hauptfleisch, A. Trautwein, V. Schünemann, *Angew. Chem. Int. Ed. Engl.* **38** (1999) 3238
10. A. Müller, M. Luban, C. Schröder, R. Modler, P. Kögerler, M. Axenovich, J. Schnack, P. C. Canfield, S. Bud'ko, N. Harrison, *Chem. Phys. Chem* **2** (2001) 517
11. J. Schnack, M. Luban, R. Modler, *Europhys. Lett.* (2001), submitted
12. E. H. Lieb, T. Schultz, D. C. Mattis, *Ann. Phys. (N.Y.)* **16** (1961) 407
13. E. H. Lieb, D. C. Mattis, *J. Math. Phys.* **3** (1962) 749
14. J. Richter, N.B. Ivanov, A. Voigt, K. Retzlaff, *J. Low Temp. Phys.* **99** (1995) 363